Synthesis of ZrO$_2$ Nanopowder using High Energy Ball Mill and Characterization

R. K. Goyal[*], S.P. Deshpande, S.S. Singare

Department of Metallurgy and Materials Science, College of Engineering, Pune – 411 005, India.

Article history	Abstract
	The work deals with synthesis of zirconia (ZrO$_2$) nanopowder from commercial micron sized ZrO$_2$ powder using high energy ball mill and its characterization using scanning electron microscopy (SEM), X-ray diffraction (XRD) and laser particle size analyzer. SEM showed a decrease in particle size from more than few micrometers to less than 50 nm when the milling time increased from 0 to 20 h. The milled powder has almost spherical shaped morphology after milling time of 15 h. XRD also showed that milled ZrO$_2$ powder has a mixture of monoclinic and tetragonal phases. XRD showed that the crystallite size decreases to 50 nm, 34 nm and 29 nm after milling for 10 h, 15 h and 20 h, respectively which was confirmed by laser particle size analyzer. Final milled ZrO$_2$ powders showed bimodal particle size distributions with mean particle size of 11 nm and 39 nm.

Introduction

Zirconium oxide (ZrO$_2$) is one of the important ceramic because of its excellent electrical, thermal, mechanical and optical properties. These properties made it a good choice for applications such as thermal barrier coating, catalyst, structural solid oxide fuel cell electrolyte, semiconductor, and structural materials. Micro- and nanosized powders of ZrO$_2$ have been synthesized by a number of methods such as precipitation [1], sol-gel method [2], combustion [3], inert gas condensation [4], and thermal decomposition of zirconium complexes [5]. The high energy ball milling (or planetary ball mill) has been successfully used for the synthesis of nanopowders of PbZr$_{1-x}$TixO$_3$, Sr$_{0.8}$Bi$_{2.2}$Ta$_2$O$_9$ [6,7], zinc oxide [8], iron [9], silicon carbide [10], Nd$_2$Fe$_{14}$B/Sm$_2$Co$_{17}$ [11], LiNbO$_3$[12] etc. This technique is known to be simple, cost-effective and suitable for large scale production of nanopowders. Nevertheless, owing to high surface area to volume ratio nanoparticles provide good interface with the polymer matrices such as polystyrene [13], polymethylmethacrylate [14], polyvinylidene fluoride [15] and epoxy [16]. Recently, Zakeri et al. [17] reported a synthesis of nanostructure tetragonal ZrO$_2$ using high energy ball milling for 80 h but particle size distribution (quantitative) was not reported. Moreover, it is true that such (i.e., 80 h) prolonged milling time adds cost and introduces large quantity of impurity in the milled powder due to wear of balls and vials [18]. In view of this, this paper focuses on the synthesis of ZrO$_2$ nanopowder using a planetary ball mill up to 20 h in dry condition followed by characterization of the synthesized powders for morphology and crystallite/particle size. The lowest particle size obtained by laser particle size analyzer is 11 nm which is interesting.

Experimental

Commercial grade ZrO$_2$ powder purchased from Riedel-De Haen, A.G. Seelze-Hannover was used for reducing its size to nanometer scale. Its ball milling was carried out in a planetary ball

mill (PM 200, Retsch) using vials and balls made of ZrO$_2$ in dry air atmosphere. The ball to powder ratio (BPR) of 10:1 and the rotational speed of 300 rpm were maintained. The milling time was varied from 5 h to 20 h and the milled powders were analysed after every 5 h. Ball milled ZrO$_2$ powders were analysed using X-ray diffractometer (XRD, Philips X'Pert PANalytical PW 3040/60) using monochromatic CuK$_\alpha$ radiation over a 2θ angle from 10° to 90°. Crystallite size was determined from the peak broadening using the Scherrer equation (1) after subtracting instrumental broadening. The strain broadening (due to lattice strain) has been ignored here, because we have interest in determining the trend of change of crystallite size with increasing milling time.

$$d = \frac{0.9\lambda}{\beta_c \cos \theta} \qquad (1)$$

$$and \ \beta_c = \sqrt{\beta_n^2 - \beta_m^2}$$

where, β_c is corrected peak broadening (in radian) from nanopowder, β_n is the peak broadening due to nanosized powder and β_m the peak broadening from the bulk ZrO$_2$ powder. The λ is the wavelength of X-ray and θ is the Bragg angle.

The morphology and qualitative particle size distribution of ZrO$_2$ powders were studied using field emission scanning electron microscope (FE-SEM, Hitachi- S4800). The differential particle size distribution of ZrO$_2$ powders was obtained using laser particle size analyzer (LA-960, USA) using the standard test method as prescribed by manufacturer. For this, fraction of mg quantity of ZrO$_2$ powder was suspended in an ethanol solvent using ultrasonic bath for 10 min. Suspended ZrO$_2$/ethanol solution was filled in a standard sample holder and kept inside the instrument. The suspended sample is scanned with a laser beam using a rotating

---

Corresponding author. Tel.: Tel.: +91-20-25507275, Fax: +91-20-25507299
E-mail address: rkgoyal72@yahoo.co.in

wedge prism. Light scattering occurs when particles in a sample are bathed in the oscillating laser beam.

Results and Discussion

Figure 1 shows XRD pattern of as received and milled ZrO_2 powders. The XRD pattern of the powder milled for 10 h, 15 h and 20 h was shifted upwards by 1000, 2000 and 3000 a.u., respectively. Diffraction peak positions (2θ) of 0 h, 15 h, and 20 h milled powder were observed at 28.63^o, 31.77^o, 34.42^o and 35.52^o which corresponds to diffraction planes of $(11\bar{1})$, (111), (002) and (020), respectively [19]. A slight shift in the 2θ peak positions of the XRD pattern for the 10 h milled sample was observed, i.e., 2θ values were observed at 28.36^o, 31.66^o, 34.31^o, 35.63^o. By comparing with standard files of JCPDS, the milled ZrO_2 powders were found a mixture of monoclinic and tetragonal phases. The 10 h milled ZrO_2 powder has higher content of tetragonal phase, compared to other samples. Moreover, there is a significant increase in peak broadening and a decrease in peak intensity with increasing milling time. From these peaks broadening, the grain/crystallite size of various powders was determined from the Scherrer equation (1). It was found that the average grain/crystallite size decreases to 50 nm, 34 nm and 29 nm after milling time of 10 h, 15 h and 20 h, respectively.
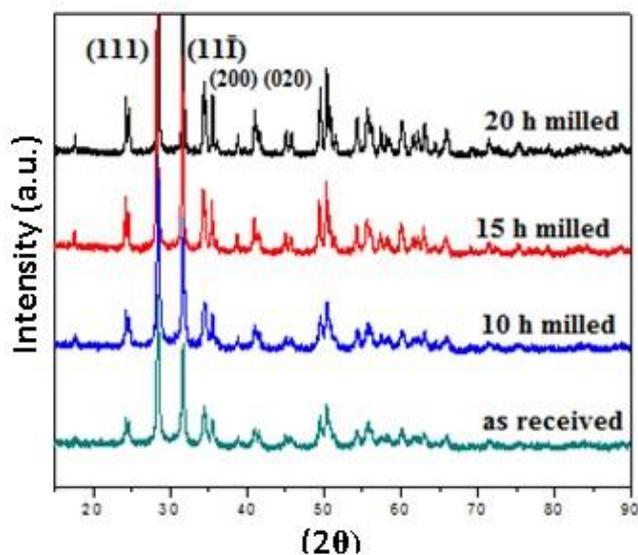

Figure 1: XRD pattern of ZrO_2 powders milled for various duration.

Figures 2(a)-(c) show SEM images of ZrO_2 powder obtained after ball milling time of 0, 10 h, and 15 h, respectively. As shown in Figure 2a, as received ZrO_2 powder shows particle size of 200-500 nm which are agglomerates of primary particles with size of more than 100 nm. After 10 h milling time, the shape of the particles looks like cuboids with length of less than 500 nm and thickness less than 60 nm. After milling time of 15 h, particle shape is almost spherical with size less than 100 nm. However, for a sample milled for 20 h (image not shown) no significant difference in size was observed probably due to the formation of agglomerates.

Figures 3(a)-(d) show particle size distribution (intensity versus size) for as received, 10 h, 15 h and 20 h milled ZrO_2 powder, respectively. Each histogram shows broader particle distribution and two peaks indicating bimodal particle size distribution. First peak indicates primary ZrO_2 particles and the second peak indicates larger size particles or aggregates of primary crystallites. Mean particle size obtained from the second peak after 0 h, 10 h, 15 h and 20 h milling time was approximately 281 nm, 65 nm, 44

nm and 39 nm, respectively. This clearly indicates that particle size was decreased significantly by planetary ball milling. Similarly, the mean particle size obtained from the first peak of histogram after 0 h, 10 h, 15 h and 20 h milling time was 53 nm, 19 nm, 15 nm and 13 nm respectively.
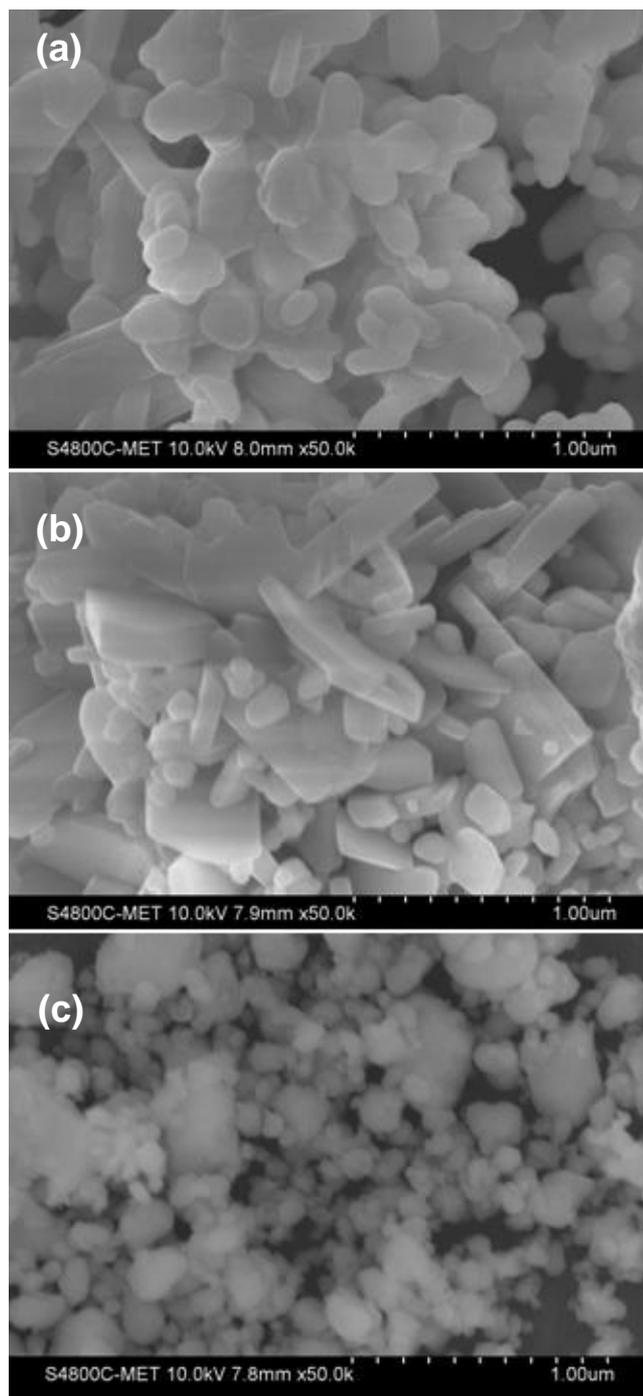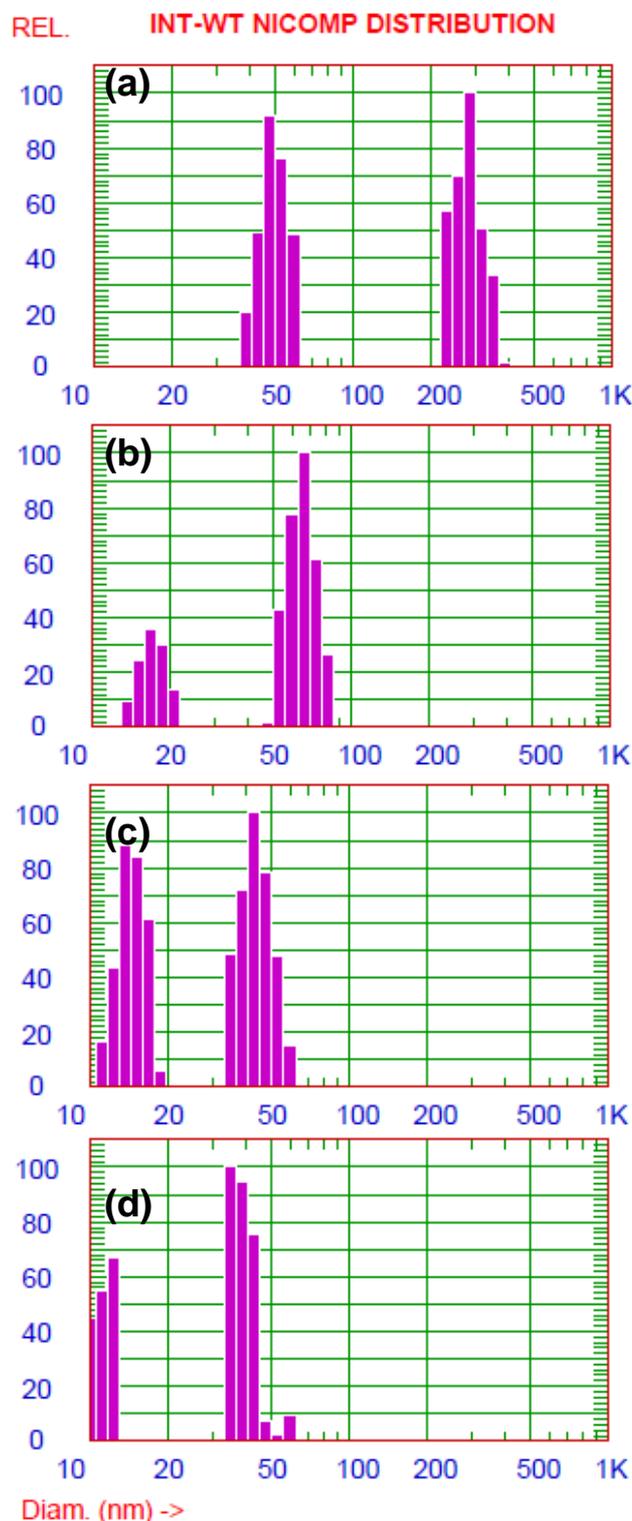

Figure 2: SEM images of ZrO_2 powder after milling time of (a) 0 h, (b) 10 h, and (c) 15 h.

The variation of corresponding crystallite and particle size determined by XRD and laser particle size analyzer, respectively, as a function of the milling time is shown in Figure 4. As shown in this Figure, crystallite and particle size first decreases sharply and then gets saturation after 15 h. In initial stage, high energy of planetary ball mill ruptures the interatomic bonds in the crystal and forms new surface. However, after a critical milling time (i.e., 15 h in present case) or when the size reached to a critical size the
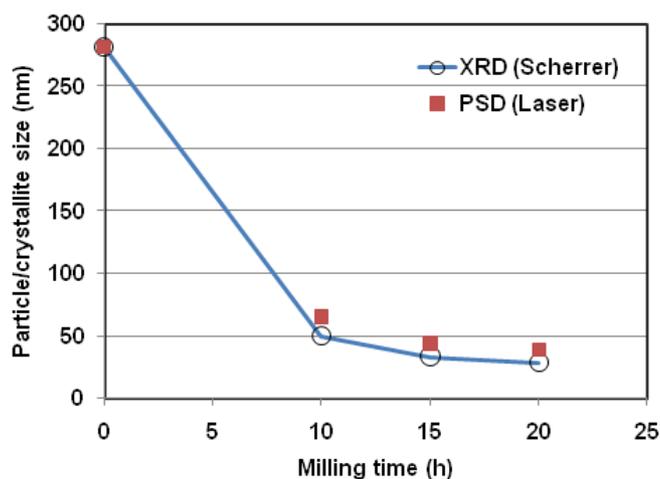
surface to volume ratio of the particles and hence their surface energy increases significantly which may lead to formation of agglomerates.

Figure 3: Particle size distribution of ZrO₂ powder after milling time of (a) 0 h, (b) 10 h, (c) 15 h and (d) 20 h.

In other words both these factors, i.e., reducing particle's sizes with increasing milling time due to high impact energy of balls and reducing surface energy by making agglomerate, competes each other and hence, particles get saturation after a critical particle size. The mean particle size obtained by the particle size analyzer is lower as well as higher than the average crystallite size obtained by

XRD peak broadening. It is due to the fact that X-ray peak broadening method is most appropriate for the crystallite sizes in the range of 10-100 nm. Moreover, particle size analyzer measures the particle size whereas XRD measures crystallite size (i.e., primary particle size or single crystal). It is also well known that the particles may be made up of a number of crystallites. In present study, particle size obtained from first peak of histogram is smaller than that of crystallite size obtained by XRD. This discrepancy may probably be attributed to the less number of much smaller sized particles which are detected by laser particle size analyzer because the intensity of the diffracted laser beam is proportional to sixth power of the particle size. In contrast, x-ray beam is less sensitive for the smaller size crystallites (< 10 nm) due to the amorphous layer on the surface.

Figure 4: Particle/crystallite size versus ball milling time for ZrO₂ powder.

Conclusions

ZrO₂ nanopowders were successfully synthesized using a planetary ball mill in dry condition. The size of particle/crystallite decreases with increasing milling time under the similar conditions. The lowest crystallite particle size obtained was 13 nm but after milling time of 15 h there was no decrease in crystallite size. SEM indicated almost spherical shaped morphology of the milled powder. As received as well as milled ZrO₂ powders showed bimodal particle size distributions and their peak positions of the histograms shifted towards lower size with increasing milling time.

References

1. Tyagi, B.;Sidhpuria, K.; Shaik, B.; JasraR.V.; Ind. Eng. Chem. Res. 2006,45,8643-8650. **DOI:** 10.1021/ie060519p.
2. Heshmatpour, F.; Aghakhanpour R.B.; Powder Technology. 2011,205,193-200. DOI:10.1016/j.powtec.2010.08.299
3. Purohit, R.D.; Saha S.; Tayagi, A.K. Mater. Sci. Eng. B. 2006,130,57-60. DOI:10.1016/j.mseb.2006.02.041
4. Nitsche, M.; Rodewald, M.; Skandan G.; Fuess, H.; Hahn H.; Nanostruct. Mater. 1996,7,535-546. DOI:10.1016/0965-9773(96)00027-X
5. Salavati-Niasari, M.; Dadkhah, M.; Davar, F. Inorg. Chim. Acta 2009,362, 3969-3974.DOI: 10.1016/j.ica.2009.05.036
6. Nath, A.K.; Singh, J.K.; Physica B. 2010, 405, 430–434. DOI:10.1016/j.physb.2009.08.299

7. Sugandha; Jha, A.K.; Materials Characterization 2012, 65, 126 – 132. DOI: 10.1016/j.matchar.2011.12.011.

8. Amirkhanloun, S.T.; Ketabchi, M.P.; Parvin, N.D.; Materials Letters 2012,86, 122 – 124. DOI: 10.1016/j.matlet.2012.07.041

9. Goyal, R.K.; Dhoka, P.; Bora, A.; Gaikwad, P.; Journal of Materials Science & Surface Engineering, 2016, 4(1), 339-341.

10. Rao, J.P.; Kush, D.H.; Bhargava, N.M.; Journal of Minerals & Materials Characterization & Engineering 2012 11, 529 - 541. DOI: 10.4236/jmmce.2012.115038.

11. Indris, S.S.; Bork, D.; Heitjans, P.; Journal of Materials Synthesis and Processing 2000, 8(3), 245 - 250. DOI: 10.1023/A:1011324429011.

12. Poudyal, N.; Altuncevahir, B.; Chakka, V.; Chen, K.; Black, T.D.; Liu, J.P.; Ding, Y.; Wang, Z.L.; J Phys. D: Appl. Phys. 2004, 37, L45 - L48. DOI:10.1088/0022-3727/37/24/L01.

13. Goyal, R.K.; Tiwari, A.N.; Mulik, U.P.; Negi, Y.S.; J. Phys. D: Appl.Phys. 2008, 41, 85403. DOI:10.1088/0022-3727/41/8/085403.

14. Goyal, R.K.; Katkade, S.S.; Mule, D.M.; Composites: Part B 2013, 44, 128 – 132. DOI: 10.1016/j.compositesb.2012.06.019

15. Mendes, S.F.; Costa, C.M.; Caparros, C.; Sencadas, V.; Lanceros-Mendez, S.; J. Mat. Sci. 2010, 47, 1378 – 1388. DOI: 10.1007/s10853-011-5916-7.

16. Yang, W.; Yu, S.; Luo, S.; Sun, R.; Liao, W.; Wong, C.; Journal of Alloys and Compounds 2015, 620, 315-323. DOI: 10.1016/j.jallcom.2014.09.142.

17. Zakeri M., Rahimipour M. R. and Abbasi B. J., Materials Technology, 2013, 28(4), 181-186.

18. Suryanarayana, C.; Progress in Materials Science 46 (2001) 1-184. DOI:10.1016/S0079-6425(99)00010-9.

19. Srinivasan, R.; Angelis, R.J.; Ice, G.; B. Davis, H. Journal of Materials Research 1991,6,1287-1292. DOI: http://dx.doi.org/10.1557/JMR.1991.1287.